

Letters

Ultra-compact, High-Frequency Power Integrated Circuits Based on GaN-on-Si Schottky Barrier Diodes

Luca Nela ¹, Student Member, IEEE, Remco Van Erp ², Georgios Kampitsis ³, Member, IEEE, Halil Kerim Yildirim ⁴, Jun Ma ⁵, and Elisa Matioli ⁶, Member, IEEE

Abstract—Gallium nitride (GaN) transistors are being employed in an increasing number of applications thanks to their excellent performance and competitive price. Yet, GaN diodes are not commercially available, and little is known about their performance and potential impact on power circuit design. In this article, we demonstrate scaled-up GaN-on-Si Tri-Anode Schottky barrier diodes (SBDs), whose excellent dc and switching performance are compared to commercial Si fast-recovery diodes and SiC SBDs. Moreover, the advantageous lateral GaN-on-Si architecture enables the integration of several devices on the same chip, paving the way for power integrated circuits (ICs). This is demonstrated by realizing a diode-multiplier IC, which includes up to eight monolithically integrated SBDs on the same chip. The IC was integrated on a dc–dc magnetic-less boost converter able to operate at a frequency of 1 MHz. The IC performance and footprint are compared to the same circuit realized with discrete Si and SiC vertical devices, showing the potential of GaN power ICs for efficient and compact power converters.

Index Terms—Diode multiplier, gallium nitride (GaN), GaN-on-Si, GaN diode, Tri-Anode, power integrated circuit (IC).

I. INTRODUCTION

GALLIUM nitride (GaN) has emerged as a promising material platform for low to medium power applications thanks to its excellent electronic properties [1], [2]. GaN transistors are already available on the market, showing comparable performance to silicon carbide (SiC) devices at a potentially more competitive price thanks to the low-cost and large-area GaN-on-Si technology, which is overcoming its technical challenges and becoming more mature. In addition, while typical power integrated circuits (ICs) based on bipolar-CMOS-DMOS (BCD) technology [3] show inferior performance with respect

Manuscript received May 26, 2020; revised June 23, 2020; accepted July 3, 2020. Date of publication July 9, 2020; date of current version September 22, 2020. This work was supported in part by the European Research Council under the European Union's H2020 Program/ERC under Grant 679425, in part by the Swiss Office of Energy under Grant SI501568-01, and in part by the Swiss National Science Foundation under Assistant Professor (AP) Energy Grant PYAPP2_166901. (Corresponding author: Luca Nela.)

The authors are with the Power and Wide-Band-Gap Electronics Research Laboratory, École Polytechnique Fédérale de Lausanne, 1015 Lausanne, Switzerland (e-mail: luca.nela@epfl.ch; remco.vanerp@epfl.ch; gkampit@gmail.com; halil.yildirim@epfl.ch; eejma@outlook.com; elison.matioli@epfl.ch).

Color versions of one or more of the figures in this article are available online at <https://ieeexplore.ieee.org>.

Digital Object Identifier 10.1109/TPEL.2020.3008226

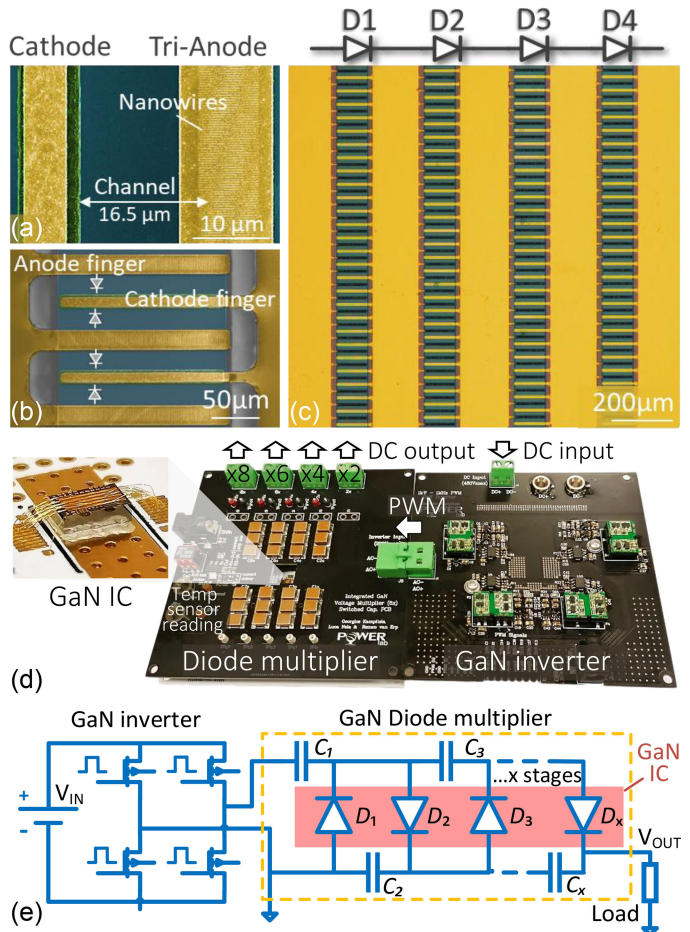


Fig. 1. SEM image of the (a) Tri-Anode SBD channel region and (b) multi-finger scaled-up device. (c) Optical microscope image of the 4-stage diode multiplier IC. (d) PCB testing setup for the diode multiplier IC which includes an inverter to generate the PWM signal and the capacitors for the voltage boosting. In the left-hand inset, a picture of the wire-bonded chip is shown. (e) Circuit schematics of the dc–dc magnetic-less boost converter. The capacitance value of the multilayer capacitors C_1 , C_2 , C_3 has been set to 6.6 μF from simulation of the circuit.

to the corresponding discrete vertical devices, the AlGaIn/GaN intrinsic lateral architecture enables straightforward integration of several high-performance components on the same chip. This paves the way for power GaN ICs that would result in lower

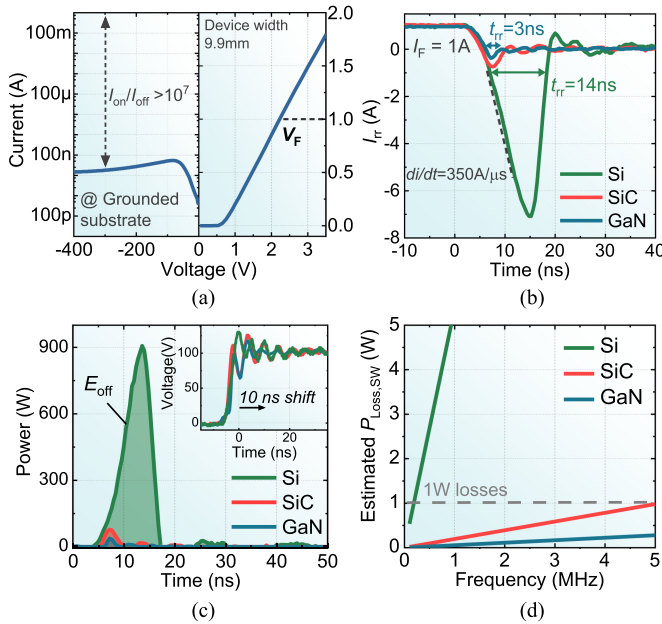


Fig. 2. (a) I - V curve for the Tri-Anode devices. (b) Reverse-recovery measurement comparing GaN Tri-Anode SBDs, Si FRDs, and SiC diodes. The reverse voltage was set to -100 V, di/dt to 350 A/ μ s, and the forward current in the ON-state to 1 A. (c) Instantaneous power loss at the diode turn-OFF and corresponding dissipated energy E_{off} . The current and voltage-probe synchronization was achieved by applying a 10 -ns correction (inset). (d) Estimated diode switching losses as a function of frequency obtained from the device E_{off} .

parasitic components, higher operating frequency, and further cost reduction.

While the development of GaN high-electron-mobility transistors (HEMTs) has been relatively fast since their first demonstration [4], GaN SBDs have encountered a more difficult path to commercialization. Among the few challenges in these devices, the difficult management of the high electric fields at the Schottky barrier results in large leakage current and poor breakdown voltage. Yet, the development of high-performance SBDs is an important requirement for a widespread adoption of GaN devices for power applications. On one side, discrete GaN SBDs would provide a competitive alternative to SiC devices in terms of performance and cost. On the other side, the integration of multiple GaN SBDs and HEMTs on the same chip would significantly expand the design possibilities, enabling power ICs with a large variety of topologies and able to operate at high frequency. In particular, the increased switching frequency represents a key advantage for converter architectures based on switching capacitors, in which no magnetic components are needed, as this would enable higher power transfer with reduced passive component size, leading to ultra-compact, high-efficiency power converters [5], [6]. Possible applications that would highly benefit from such features, and operate in the few hundreds of Watts range, include photovoltaics, lighting and robotics, among others [7].

Recently, novel device architectures such as recessed anode [8]–[10], multiple field plates [11], [12], and Tri-Gate/Tri-Anode hybrid structures [13]–[15] have enabled major improvements in GaN SBDs R_{ON} versus V_{BR} figure of merit, resulting in excellent dc behavior with low turn-ON voltage (V_{ON}) and good

TABLE I
COMPARISON OF Q_{rr} , E_{off} , AND $V_F \cdot Q_{rr}$ EXTRACTED FROM Fig. 2 FOR THE GaN TRI-ANODE DEVICES AND THE REFERENCE Si FRD AND SiC SBD

	Si FRD	SiC SBD	GaN Tri-Anode
Q_{rr} [nC]	51	2.1	0.6
E_{off} [μ J]	5.4	0.2	0.056
$V_F \cdot Q_{rr}$ [V \cdot nC]	127.5	3.36	1.4

The forward voltage V_F has been defined at a current of 1 A.

reverse-blocking capability. Yet, few works have focused on their dynamic performance and their comparison with counterpart Si and SiC devices. In addition, the GaN SBD behavior and performance in real circuit applications are still largely unexplored.

In this article, we present a thorough switching characterization of Tri-Anode GaN diodes, which are compared to similarly rated Si fast-recovery diodes and SiC SBDs. The device turn-OFF losses are evaluated through a reverse-recovery measurement, highlighting the excellent dynamic behavior of GaN SBDs. The potential of the presented diodes for high-frequency power application is demonstrated by integrating eight diodes on the same chip, to realize a monolithically integrated diode multiplier operating at 1 MHz and able to provide up to eightfold multiplication of the input voltage. The GaN IC performance is compared to the same circuit realized by discrete Si and SiC commercial devices, showing a significant improvement in high-frequency operation along with a large size reduction.

II. FABRICATION AND EXPERIMENTAL SETUP

The GaN Tri-Anode diodes and the monolithically integrated ICs were fabricated on a 6-inch GaN-on-Si heterostructure consisting of 4.2 μ m of buffer, 420 nm of unintentionally doped GaN (u-GaN) channel, 20 nm of $Al_{0.25}Ga_{0.75}N$ barrier, and 2.9 nm of u-GaN cap-layer. The detailed fabrication steps are reported in [16]. Scaled-up devices were achieved by a multi-finger approach, paralleling 50 fingers for a total device width of 9.9 mm. The diode multiplier IC was realized by properly interconnecting 4–8 diodes on the same chip [see Fig. 1(a)–(c)]. The GaN IC was combined with a GaN inverter circuit to realize a dc–dc boost converter [see Fig. 1(d)]. The input dc signal is converted into a pulswidth modulated (PWM) signal by the full-bridge inverter, and then, amplified and rectified by the diode multiplier IC and output capacitors. The voltage amplification depends on the number of stages (in this case $\times 4$, $\times 6$, and $\times 8$ outputs are available). An integrated on-chip temperature sensor was included, whose value is read through a current mirror circuit. The complete circuit schematics are presented in Fig. 1(e).

III. RESULTS AND DISCUSSION

The individual Tri-Anode GaN SBD I - V shows forward voltage (V_F) of 2.2 V at a current I_F of 1 A and ON/OFF ratio higher than 10^7 at a reverse voltage V_R of -400 V [see Fig. 2(a)]. Such good dc performance is in agreement with our previous works

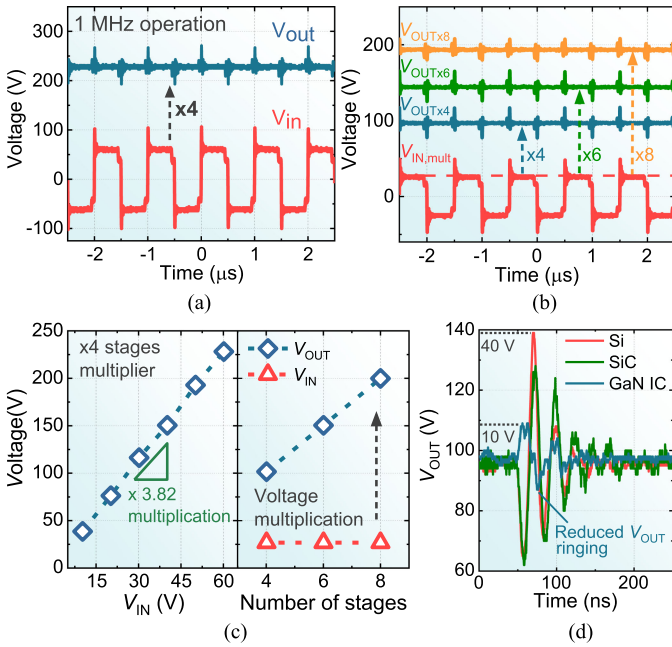


Fig. 3. (a) Operation of the 4-stage diode multiplier IC for input signal frequency of 1 MHz. (b) Output voltage for the same V_{IN} for a 4-, 6-, and 8-stage diode multiplier. (c) V_{OUT} as a function of V_{IN} for a 4-stage diode multiplier (left) and as a function of the number of stages for the same V_{IN} (right). (d) V_{OUT} ringing comparison for a diode multiplier realized with the presented GaN IC and by discrete Si and SiC reference devices.

on the subject [13], [14]. To characterize the SBD switching performance and evaluate the losses associated with its turn-OFF, a double-pulse-tester (DPT) measurement was performed. Fig. 2(b) shows the Tri-Anode SBD reverse-recovery behavior, which is compared to a commercial Si fast-recovery diode (FRD) [17] and SiC SBD [18] with a similar rating. The Tri-Anode GaN SBD significantly outperforms the Si device in terms of reverse-recovery time (t_{rr}), current (I_{rr}), and overall charge (Q_{rr}), and compares well to the SiC device. Such improvements come from the superior AlGaIn/GaN material properties for power applications, such as high electron mobility and large critical electric field, combined with the excellent Tri-Anode architecture [16]. The total reverse-recovery charge for the three devices, obtained from the time-integration of I_{rr} , is reported in Table I, which also shows a significant improvement in the $Q_{rr} \cdot V_F$ figure-of-merit for the GaN Tri-Anode devices. To extract the losses associated with each diode turn-OFF event, the voltage over the diode during the reverse-recovery measurement was recorded and multiplied point-by-point by I_{rr} to obtain the instantaneous power loss. Calibration of the voltage and current probes over a resistive load was performed to ensure a synchronous measurement. Fig. 2(c) shows a comparison of the instantaneous diode power loss at each turn-OFF, highlighting a large peak for the Si FRD and a much-reduced value for the SiC and GaN SBDs. By time-integrating the power peak of Fig. 2(c), it is possible to extract the switching energy loss (E_{off}) at each cycle (see Table I) and thus, estimate the switching losses for the three devices at different frequencies. From Fig. 2(d), it is clear that the Si FRD cannot operate above few hundreds of kHz

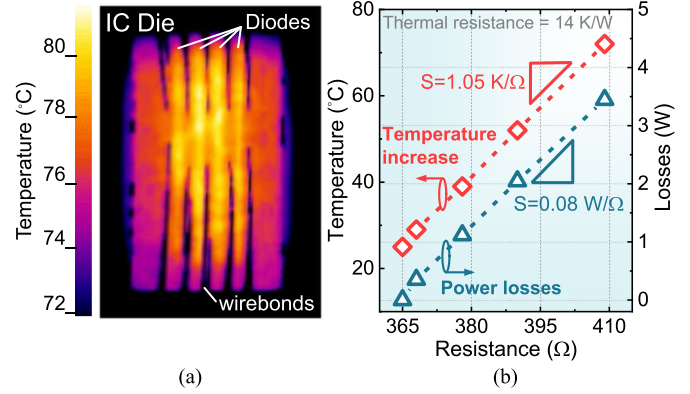


Fig. 4. (a) Thermal image of the 4-diode multiplier IC during operation obtained using a FLIR SC3000 IR camera. A uniform emissivity was obtained by coating the device surface with black paint. (b) Integrated sensor calibration with the IC temperature and the IC dissipated power, showing good linearity and a sensitivity of $S_{th} = 1.05 \text{ K}/\Omega$ and $S_P = 0.08 \text{ W}/\Omega$, respectively.

without significant switching losses, while, as expected, the SiC and GaN SBD represent a suitable solution for the MHz range.

The promising performance from the single-diode characterization was applied to a real circuit application, as a diode multiplier, able to perform dc-dc boost conversion. To this end, four to eight of the presented Tri-Anode GaN diodes were monolithically integrated on the same chip to realize the desired IC, which was tested using the setup shown in Fig. 1(d). Fig. 3(a) demonstrates the operation of the 4-diode circuit which is able to boost and rectify the input PWM signal generated by the inverter into a dc output (V_{OUT}). The circuit operating frequency is 1 MHz. An important advantage of the diode multiplier topology is its modularity which allows to easily enhance the V_{OUT} multiplication factor by increasing the number of stages. Each stage is composed of two diodes and two capacitors [see Fig. 1(e)]. Fig. 3(b) reports the output voltage for a diode multiplier with 4, 6, and 8 stages at the same V_{IN} , successfully showing an increase in the boosting ratio. Fig. 3(c) shows V_{OUT} as a function of V_{IN} for a four-diode multiplier (left) and as a function of the number of stages for the same input voltage (right). The multiplication factor for the four-diode multiplier is 3.82, slightly lower than the theoretical value of 4 due to the losses over the four diodes. The shorter interconnections and lower parasitic contribution from the GaN IC result in an important decrease of the output voltage ringing and overshoot with respect to the reference circuit realized with Si or SiC discrete devices [see Fig. 3(d)]. It should be noted that the 1-MHz operating frequency was chosen to comply with the capacitor and inverter specifications and was not limited by the GaN IC, which could operate at higher frequencies.

While power ICs can significantly enhance the power density, careful thermal management solutions and temperature monitoring are of extreme importance to deal with such high heat fluxes. A continuous, near-junction temperature tracking is important to avoid device overheating, increase its reliability, and monitor its losses. To this end, an on-chip sensing resistor [19] was designed in close proximity to the GaN IC to control its temperature during operation. By monitoring the IC temperature with a thermal

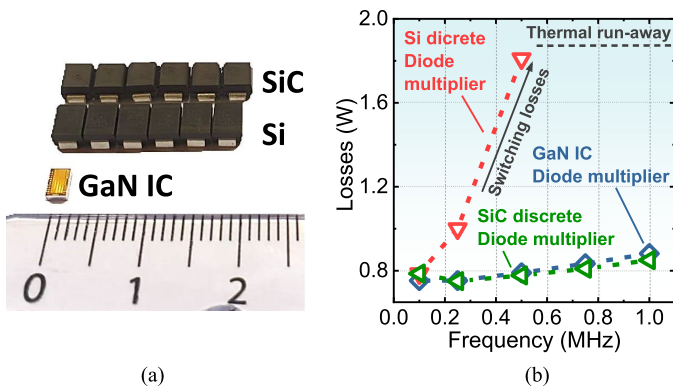


Fig. 5. (a) Size comparison for the Tri-Anode GaN-on-Si 6-stage diode multiplier ICs with respect to the same circuit realized with discrete vertical surface-mounted Si and SiC devices. (b) Losses as a function of frequency for the GaN IC and the reference circuits made of Si and SiC discrete devices. The losses were evaluated at a constant output power by thermal measurement.

camera [see Fig. 4(a)] and simultaneously measuring the resistor value, the temperature sensor was calibrated, resulting in a sensitivity of $1.05 \text{ K}/\Omega$ [see Fig. 4(b)]. In addition, by connecting the diodes in series and dissipating a known dc power over the IC, the sensor resistance was linked to the IC dissipated power to extract the device thermal resistance. This enables, after proper calibration, continuous monitoring of the IC losses during its operation with a simple electrical measurement.

The diode multiplier GaN ICs were compared to the same circuit realized by Si and SiC discrete devices. Thanks to its lateral architecture, AlGaN/GaN devices can be easily integrated on the same chip to realize power ICs. However, this is not the case for Si and SiC devices whose vertical device architecture requires the use of discrete components or sophisticated and expensive back-end techniques to copackage multiple devices together. This results in a drastic size reduction and power density increase for GaN ICs, in which six power diodes could be integrated in a chip size of $2.3 \text{ mm} \times 3.6 \text{ mm}$, leading to more than ten times reduction in footprint with respect to similarly rated surface-mounted Si and SiC discrete diodes [see Fig. 5(a)]. In addition, the reduction of the interconnection parasitics thanks to the ICs monolithic integration enables high-frequency operation with minimum ringing and overshoot voltage, as seen in Fig. 3(d).

Fig. 5(b) shows the losses as a function of the operating frequency for 4-stage diode multipliers realized with discrete Si FRDs, SiC SBDs, and the GaN ICs at the same output power. The losses for all devices were extracted from thermal measurement by IR camera. While the different diodes were chosen to have similar V_F and current rating, and thus show comparable conduction losses, the total loss contribution as a function of the frequency strongly depends on the device technology. In particular, the diode multiplier realized with Si diodes shows a rapid loss increase as the frequency is raised. Such a trend is due to the Si FRD large reverse-recovery charge, which results in a substantial energy loss at each turn-OFF event [see Fig. 2(c)]. This leads to significant switching losses, which completely dominate over conduction losses, and rapidly increase until the circuit fails due to thermal runaway. The GaN IC diode multiplier and the one

realized with SiC discrete devices show instead only a moderate loss increase from an operating frequency of 100 kHz to 1 MHz, benefiting from the much-reduced diode E_{off} with respect to the Si devices [see Fig. 2(c)]. In this case, conduction losses, which are constant in frequency, represent the main contribution. The behavior of the different diode multiplier circuits agrees well with the single-diode switching performance characterization shown in Fig. 2. Thanks to the reduced switching losses, the GaN IC is able to properly operate in the MHz range with minimum loss increase. Such high operating frequency, combined with the reduced ringing from the IC design, is very promising for switching-capacitor architectures since it allows to reduce the overall capacitor value and size, and to significantly increase the converter output power.

IV. CONCLUSION

In this article, we presented the promising potential of Tri-Anode GaN-on-Si SBDs for future high-frequency power applications. The results from the Tri-Anode lateral diodes significantly outperform Si FRD and are comparable with SiC SBDs. In addition, thanks to the lateral architecture, Tri-Anode devices can be monolithically integrated to realize power ICs able to operate at high frequency, thanks to the reduced diode switching losses and low interconnection parasitics. This is demonstrated by realizing a diode multiplier IC that includes up to eight diodes on the same chip and is able to operate as a dc-dc magnetic-less boost converter with $\times 8$ multiplication factor at a frequency of 1 MHz, which cannot be matched by Si FRD devices. In addition, the monolithic device integration enables a significant reduction of the device footprint, which is more than ten times smaller than for Si and SiC discrete devices, paving the way for compact and cost-effective solutions. Finally, the IC platform enables the integration of an on-chip sensor for electrical, real-time monitoring of the circuit temperature and losses. These results demonstrate the promising potential of Tri-Anode GaN-on-Si SBDs for future compact, fast-switching, and cost-effective power ICs.

REFERENCES

- [1] K. J. Chen *et al.*, "GaN-on-Si power technology: Devices and applications," *IEEE Trans. Electron Devices*, vol. 64, no. 3, pp. 779–795, Mar. 2017.
- [2] H. Amano *et al.*, "The 2018 GaN power electronics roadmap," *J. Phys. D: Appl. Phys.*, vol. 51, no. 16, 2018, Art. no. 163001.
- [3] C. Contiero, A. Andreini, and P. Galbiati, "Roadmap differentiation and emerging trends in BCD technology," in *Proc. Eur. Solid-State Device Res. Conf.*, 2002, pp. 275–282.
- [4] A. Bykhovski, B. Gelmont, and M. Shur, "The influence of the strain-induced electric field on the charge distribution in GaN-AlN-GaN structure," *J. Appl. Phys.*, vol. 74, no. 11, pp. 6734–6739, 1993.
- [5] W. Qian, D. Cao, J. G. Cintron-Rivera, M. Gebben, D. Wey, and F. Z. Peng, "A switched-capacitor DC-DC converter with high voltage gain and reduced component rating and count," *IEEE Trans. Ind. Appl.*, vol. 48, no. 4, pp. 1397–1406, Jul./Aug. 2012.
- [6] G. Kampitsis, R. Van Erp, and E. Matioli, "Ultra-high power density magnetic-less DC/DC converter utilizing GaN transistors," in *Proc. IEEE Appl. Power Electron. Conf. Expo.*, 2019, pp. 1609–1615.
- [7] M. Forouzesh, Y. P. Siwakoti, S. A. Gorji, F. Blaabjerg, and B. Lehman, "Step-up DC-DC converters: A comprehensive review of voltage-boosting techniques, topologies, and applications," *IEEE Trans. Power Electron.*, vol. 32, no. 12, pp. 9143–9178, Dec. 2017.

- [8] Q. Zhou *et al.*, "High reverse blocking and low onset voltage AlGaIn/GaN-on-Si lateral power diode with MIS-gated hybrid anode," *IEEE Electron Device Lett.*, vol. 36, no. 7, pp. 660–662, Jul. 2015.
- [9] J. Lei *et al.*, "650-V double-channel lateral schottky barrier diode with dual-recess gated anode," *IEEE Electron Device Lett.*, vol. 39, no. 2, pp. 260–263, Feb. 2018.
- [10] J. Hu *et al.*, "Performance optimization of au-free lateral AlGaIn/GaN schottky barrier diode with gated edge termination on 200-mm silicon substrate," *IEEE Trans. Electron Devices*, vol. 63, no. 3, pp. 997–1004, Mar. 2016.
- [11] B. Weiss, R. Reiner, P. Waltereit, R. Quay, and O. Ambacher, "Analysis and modeling of GaN-based multi field plate Schottky power diodes," in *Proc. IEEE 17th Work. Control Model. Power Electron.*, 2016, pp. 1–6.
- [12] M. Zhu *et al.*, "1.9-kV AlGaIn/GaN lateral Schottky barrier diodes on silicon," *IEEE Electron Device Lett.*, vol. 36, no. 4, pp. 375–377, Apr. 2015.
- [13] J. Ma and E. Matioli, "High-voltage and low-leakage AlGaIn/GaN tri-anode Schottky diodes with integrated tri-gate transistors," *IEEE Electron Device Lett.*, vol. 38, no. 1, pp. 83–86, Jan. 2017.
- [14] J. Ma and E. Matioli, "2 kV slanted tri-gate GaN-on-Si Schottky barrier diodes with ultra-low leakage current," *Appl. Phys. Lett.*, vol. 112, no. 5, 2018, Art. no. 052101.
- [15] E. Matioli, B. Lu, and T. Palacios, "Ultralow leakage current AlGaIn/GaN Schottky diodes with 3-D anode structure," *IEEE Trans. Electron Devices*, vol. 60, no. 10, pp. 3365–3370, Oct. 2013.
- [16] L. Nela, G. Kampitsis, J. Ma, and E. Matioli, "Fast-switching tri-anode Schottky barrier diodes for monolithically integrated GaN-on-Si power circuits," *IEEE Electron Device Lett.*, vol. 41, no. 1, pp. 99–102, Jan. 2020.
- [17] [Online]. Available: [https://www.mccsemi.com/pdf/Products/ER1A-L~ER1J-L\(DO-214AA\).pdf](https://www.mccsemi.com/pdf/Products/ER1A-L~ER1J-L(DO-214AA).pdf)
- [18] [Online]. Available: http://www.genesicsemi.com/schottky_mps/GB01SLT06-214.pdf
- [19] R. Reiner *et al.*, "Linear temperature sensors in high-voltage GaN-HEMT power devices," in *Proc. IEEE Appl. Power Electron. Conf. Expo.*, 2016, pp. 2083–2086.